Active depinning of bacterial droplets: the collective surfing of Bacillus subtilis

Marc Hennes[a], **Julien Tailleur**[a], **Gaëlle Charron**[a], **and Adrian Daerr**[a,1]

[a]Laboratoire Matière et Systèmes Complexes (MSC) UMR CNRS 7057, University Paris Diderot, 75205 Paris cedex 13, France

This is the preprint as submitted to PNAS. For the final published version see the PNAS web site at www.pnas.org/cgi/doi/10.1073/pnas.1703997114

How systems are endowed with migration capacity is a fascinating question with implications ranging from the design of novel active systems to the control of microbial populations. Bacteria, which can be found in a variety of environments, have developed among the richest set of locomotion mechanisms both at the microscopic and collective levels. Here, we uncover experimentally a new mode of collective bacterial motility in humid environment through the depinning of bacterial droplets. While capillary forces are notoriously enormous at the bacterial scale, even capable of pinning water droplets of millimetric size on inclined surfaces, we show that bacteria are able to harness a variety of mechanisms to unpin contact lines, hence inducing a collective slipping of the colony across the surface. Contrary to flagella-dependent migration modes like swarming we show that this much faster 'colony surfing' still occurs in mutant strains of *Bacillus subtilis* lacking flagella. The active unpinning seen in our experiments relies on a variety of microscopic mechanisms which could each play an important role in the migration of microorganisms in humid environment.

Wetting | Bacterial motility | Collective motion

Collective behaviours in bacterial colonies, from swarming and bacterial turbulence (1) to biofilm (2, 3) and pattern formation (4–7), are among the most fascinating problems at the crossroads of biology, chemistry and physics. They raise fundamental questions, such as the emergence of complex behaviours from simple microscopic dynamics, and are of practical importance due to their medical impact (8). Thanks to studies carried out in simplified, controlled environments, much is known about the swimming of bacteria in three dimensional fluids (9). A lot of effort has thus been devoted over the past few years to the study of bacterial motion in more complex environments, in particular near interfaces (10–12).

A prototypical case study is the spreading of *Bacillus subtilis* colonies on the surface of agar gels (13, 14). By changing the nutrient and agar concentrations, very diverse colony morphologies are observed, ranging from simple diffusive spreading to the formation of fractal dendritic structures. The motion of bacteria on hard gel substrates vividly differs from the unconstrained swimming in liquid: isolated bacteria indeed cannot move on agar gels since their propulsion forces are much weaker than the capillary forces they experience from the surrounding liquid film. Colony migration remains possible but relies on cooperativity to overcome pinning, as in the dense mass swarming that many bacteria exhibit (15, 16).

The importance of capillary forces at small scales is familiar to us all from the observation of glass windows after the rain, or the walls of a fridge or cold storage facility, on which small drops remain stuck. A drop can indeed only slide when the driving gravitational force overcomes the capillary pinning force. Similarly, small water drops of, say, 2 µl remain stuck at the surface of an agar gel, at any tilt angle. Here we show that bacteria are able to unpin such droplets, leading in practice to the collective 'surfing' of the entire colony. Surprisingly, this happens on slopes *as small as* 0.1°, commonly encountered on any generic surface, and leads to migration speeds well above that of mass swarming.

Results

Active depinning of bacterial droplets. A 2 µl drop of a suspension of *B. subtilis* grown to an optical density OD = 0.27 is deposited on top of a 0.7 % agar gel substrate with nutrients, and incubated in a climate chamber at fixed temperature and relative humidity (T=30 °C, RH=70 %, see *Materials and Methods*). Fig. 1a and movie SM1 show the typical evolution of the drop for a gel surface inclination of $\alpha = 1°$. During the first hour, it exhibits a slight isotropic spreading, typical of aqueous surfactant solutions on hydrogels (17, 18). This is expected since our *B. subtilis* strain is known to produce *surfactin*, a cyclic lipopeptide which strongly reduces surface tension (19, 20). The surfactant also causes some swelling of the gel as it spreads outwards, producing a visible 'surfactant ring' (21) that grows radially. Around seven hours after deposition, however, the drop starts sliding in the direction of inclination. Bacteria move along with the drop as it slides, hence the name *colony surfing*. The drop velocity rapidly increases to reach $1.5\,\mathrm{cm\,h^{-1}}$, almost an order of magnitude larger than the speed of swarming of our *B. subtilis* strain on flat gels. This surfing motion persists at roughly constant drop diameter and velocity until the drop reaches the rim of the Petri dish. Interestingly, bacteria continuously exit from

Significance Statement

How bacteria propagate and colonise new environments is of paramount importance e.g. to food processing, transport and storage. In this article we show that *Bacillus subtilis* can turn millimetric water droplets into vehicles to quickly cover large distances. To this end they overcome the enormous capillary forces that prevent the sliding of water droplets even on vertical surfaces such as refrigerator walls. *B. subtilis* does so by actively unpinning the surrounding liquid to cause the collective surfing of the entire community on slopes as small as 0.1°. We show this depinning to rely on a variety of mechanisms, that could each be relevant to the motility of microorganisms in partially humid environments such as unsaturated soils.

MH, JT, GC, and AD designed research; MH and AD performed research; MH, JT, GC, and AD analysed data; MH, JT, and AD wrote the paper.

The authors declare no conflict of interest.

[1]To whom correspondence should be addressed. E-mail: adrian.daerr@univ-paris-diderot.fr

This article contains supporting information online at www.pnas.org/lookup/suppl/doi:10.1073/pnas.1703997114/-/DCSupplemental.

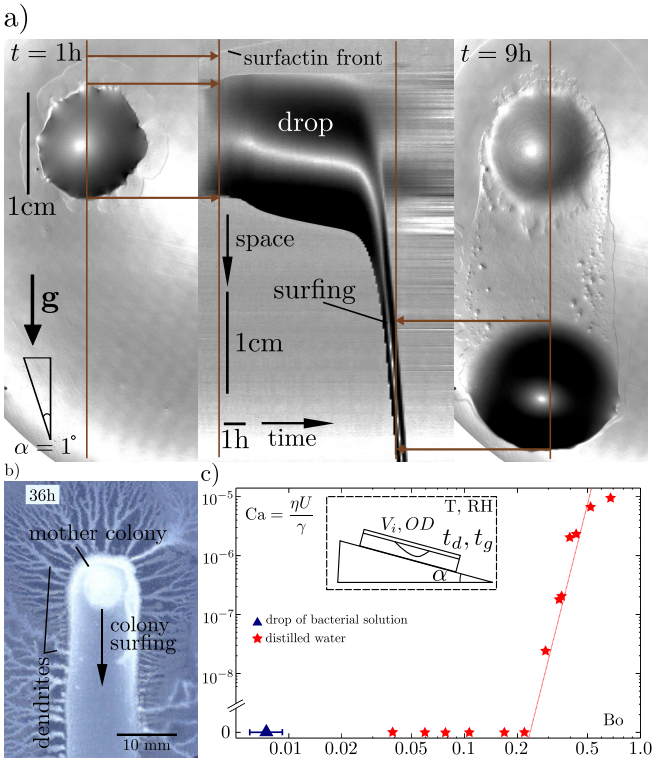

Fig. 1. a) Top view of colony surfing where grey levels indicate the local slope. A 2 µl drop is still immobile at $t = 1$ hour after its deposition (left). The onset of slipping motion at $t = 7$ hour is visible on the central kymograph which represents the time evolution of a cut through the drop along the direction of motion (brown line). The gel remains swollen around the point of deposition (upper dark region, right). **b)** 36h after deposition, the bacteria which have been carried by the sliding drop have invaded the whole drop trajectory and its surroundings. **c)** Dimensionless velocity vs gravitational pull of water drops, measured by their Capillary and Bond numbers (red stars). The initial Bond number of the bacteria-laden drop shown in (a) (0.003, blue triangle) is orders of magnitude below the critical Bond number $\mathrm{Bo}_c^{H_2O} \approx 0.25$ at which water drops start sliding.

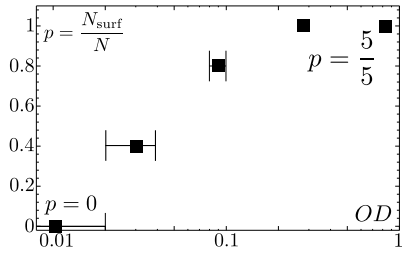

Fig. 2. Fraction of colony surfing events for different bacterial concentrations in the deposited drop. Out of five experiments, none show surfing for initial optical densities below OD $= 0.02$, while surfing always occurs at OD $= 0.27$ and above.

the drop as it slides so that they rapidly colonise the whole drop trajectory and its surrounding (Fig. 1b).

The mobility of the bacteria-laden drops is striking when compared to droplets of water or pure nutrient solution. Water droplets indeed only start sliding on slopes *two orders of magnitude larger* than bacterial droplets of the same volume. This is best quantified using the ratio of gravitational to capillary forces, using the so-called Bond number

$$\mathrm{Bo} = \frac{\rho V g \sin\alpha}{V^{1/3}\gamma} \qquad [1]$$

where ρV and $V^{1/3}$ are the drop mass and typical width, $g\sin\alpha$ the effective gravity, and γ the surface tension. We always observe the sliding of bacteria-laden droplets with an initial Bond number of $\mathrm{Bo} \simeq 3\cdot 10^{-3}$ whereas water drops only start sliding for Bond numbers larger than $\mathrm{Bo}_c^{H_2O} \approx 0.25$ (Fig. 1c). The transition from an immobile water drop to a sliding bacteria-laden one occurs continuously as the initial concentration of bacteria is varied (Fig. 2). We never observe colony surfing for bacterial densities below a threshold of OD ≈ 0.02 within the first 12 hours of recording. The *surfactin* ring is still observable, but its formation is delayed by several hours. For higher concentrations, the probability of colony surfing increases, and was observed in five out of five runs for ODs above ≈ 0.2.

The bacterial medium does not solely contain bacteria but also nutrients and bacterial products including in particular *surfactin* and exopolysaccharides. To test whether the colony surfing is really due to bacteria we remove them from an OD $= 0.27$ suspension by centrifugation and filtration, and start experiments where two drops, with and without bacteria, are deposited side by side (Fig. 3 and supplementary movie SM2). While the drop containing bacteria starts sliding after 8 h, the bacteria-free drop initially remains immobile. After 10 h, a small dendrite of bacteria contaminates the second drop, which starts sliding almost immediately (the time resolution is given by the 5 min interval at which images are taken). This highlights the role played by bacteria in our set-up. Note that contamination can also induce slipping of pure water droplets (Supplementary Fig. SF1 and movie SM3).

The role of bacterial propelling forces. The depinning of the contact line (drop perimeter) arises when driving forces exceed the capillary forces. A natural explanation of the depinning of the contact line could thus be an extra contribution to the driving force due to bacterial motion (22): the self-propelling forces combined with gravity could, together, overcome the pinning force. Active forces are also known to accelerate the relaxation of polymer networks (23). This could affect the bulk rheology of the droplet itself, modify the dynamics of gel polymer desorption near the contact line or accelerate the visco-plastic stress relaxation in its vicinity, hence affecting the contact line mobility (24, 25). Finally, active swimming strongly enhances transport and mixing within the droplet, notably of nutrients and oxygen (26), which could facilitate the collective surfing of motile colonies in comparison to non-motile ones. In order to determine whether bacterial motility has an impact on colony sliding, we compared the surfing likelihood of a motile and a non-motile strain. The strains differ only in the deletion of the *hag* gene coding for *flagellin*, the protein sub-unit required for the assembly of the flagella. As shown in Fig. 4, the fraction of surfing events is similar for both strains, showing that the collective colony surfing does not require individual motility. The sole alternative are thus a decrease of capillary forces, or an increase of the gravitational pull.

Volume increase of bacterial droplet. As surprising as it may sound, bacteria are indeed able to increase the gravitational pull exerted on the surrounding droplet, by pumping water out of the environment. We show in Fig. 5 the evolution of the drop volume, measured by means of a Moiré fringe

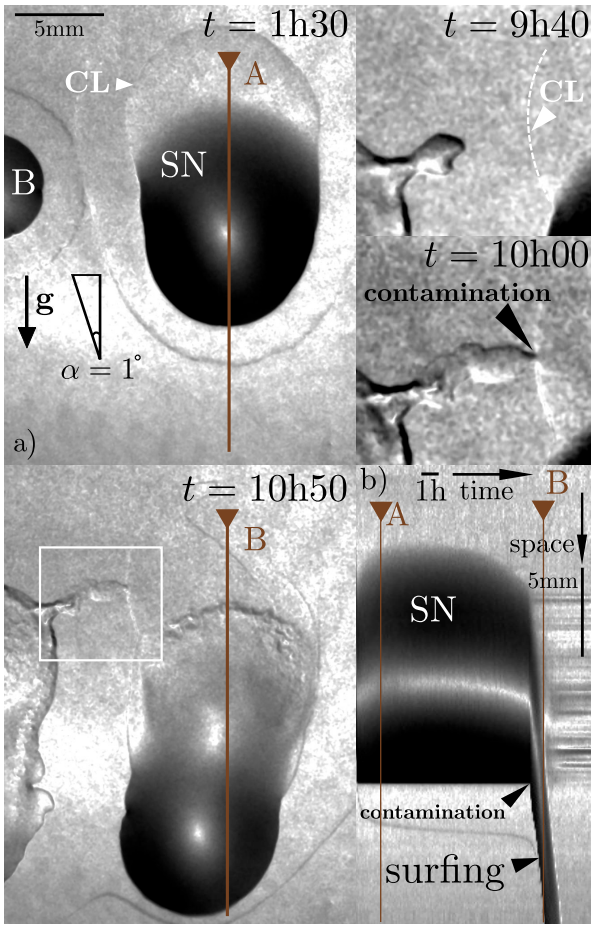

Fig. 3. a) Snapshots of induced colony surfing, where the grey-level indicates the local slope. Two drops are deposited side by side. From the right drop the bacteria were removed by centrifugation and filtration. The bacteria-laden drop (B, 1 µl) starts sliding after 8 hours while the drop containing only supernatant (SN, 10 µl) remains immobile despite its much larger volume. The magnified details at the top right (white rectangle) show how at $t \approx 10$ h, a dendrite of swarming bacteria contaminates the immobile drop (white arrow marks contact line CL), which starts sliding almost instantaneously. **b)** Kymograph of a longitudinal cut through the SN drop showing the very sudden onset of motion of the drop of supernatant after its contamination. See suppl. movie SM2.

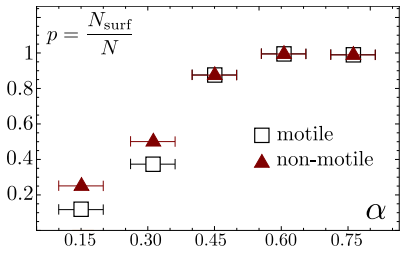

Fig. 4. Fraction of colony surfing events $p = N_{\text{surf}}/N$, out of $N = 8$ runs for each data point, for 2 µl drops (initial OD = 0.27) of a motile (SSB 1071) and non-motile (OMG 954) strain at different gel inclinations. The two strains show no statistically significant difference. The uncertainty of the tilt angle measurement is estimated to $\Delta\alpha = \pm 0.05°$.

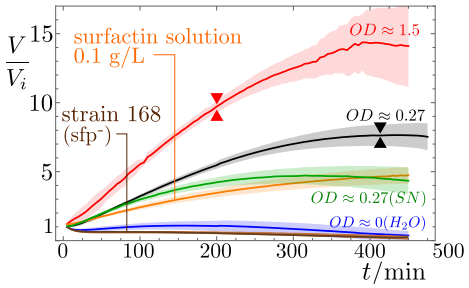

Fig. 5. Relative volume change of deposited drops of bacteria, supernatant (SN), solutions of commercial surfactin, and pure water, with respect to their deposited volume $V_i = 2$ µl. Higher bacterial optical densities at deposition result in stronger volume increase, likely because the surfactant production rate is higher. Removing the bacteria through centrifugation from an OD = 0.27 suspension and filtration just before deposition (supernatant, SN) does not affect the initial volume growth rate, but the subsequent evolution differs from the bacterial suspension (green vs. black curves). Pure *surfactin*-water drops also cause a volume increase, while no volume increase is measured for drops of pure water, nor for the non-surfactin-producing strain 168. The onset of surfing — if it occurs — is marked by double triangles. Solid lines stem from averaging over several experiments; the corresponding standard deviation is indicated by shaded areas.

deformation method (see *Materials and Methods*). Drops with a high density of bacteria show a strong volume increase prior to colony surfing. For the 2 µl drop of OD ≈ 0.27 described above, the volume grows monotonically for the first five to six hours to reach around eight times its initial value, at which point the drop starts sliding. For a higher initial concentration, OD ≈ 1.5, the drop shows a quicker volume increase, reaching a volume fifteen times its initial value and starts sliding much earlier (3.5 h after deposition).

The volume increase of pure water drops without bacteria in the same conditions is nil or negligible. On the other hand, droplets of an OD = 0.27 suspension from which bacteria are removed through centrifugation and filtration still show a significant volume increase. At this stage the supernatant (SN) solution already contains large amounts of *surfactin* (Suppl. Fig. SF9 and Table ST1), along with other products including exopolysaccharides and, of course, nutrients. A possible explanation is that the concentration gradients of chemicals produced by bacteria generate inward osmotic flows. This hypothesis is validated by the fact that drops of aqueous solution containing either pure *surfactin*, or the anionic surfactant sodium dodecyl sulfate (SDS, Fig. SF5), grow to four-to-eight times their initial volume within a four-to-seven-hour period. We believe *surfactin* to be the main responsible of these osmotic flows since the strain 168 lacking *surfactin* synthesis, because of a frameshift mutation in the *sfp* gene, is never seen to produce colony surfing at any OD, and the corresponding deposited drops do not significantly inflate (brown line in Fig. 5). This absence of volume increase also highlights the negligible role of cell division in this process. The density of bacteria indeed remains very low throughout the experiment, as we confirmed by direct measurement (Fig. SF7). Note however, that this osmotic growth is not limited to surfactants: a drop containing simply 50 % glucose also undergoes a similar volume increase (Fig. SF5). This shows that this active pumping of water from the environment could be seen beyond the sole case of surfactant-producing bacteria reported here.

Finally, note that evaporation limits the time window for colony surfing in our setup. Indeed, under the 70 % relative

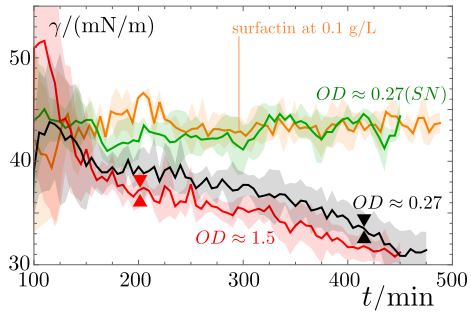

Fig. 6. The surface tension decreases monotonically over the whole duration of the experiment for drops containing *surfactin* producing bacteria. This decrease is not affected by the onset of colony surfing at $t = 205$ min for the drop of initial OD $= 1.5$, $t = 415$ min for OD $= 0.27$ (triangles). By contrast if the bacterial suspension is centrifuged and only the supernatant is deposited on the gel, the surface tension quickly becomes constant after the initial decrease due to the *surfactin* produced prior to the removal of the bacteria. A similar trend is observed for drops containing only commercial surfactin.

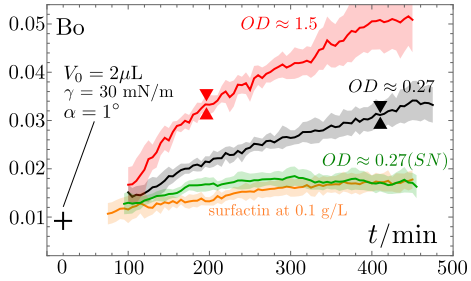

Fig. 7. The Bond number calculated using the measured volume and surface tension (Figs. 5 and 6) exhibits a monotonically increase for *surfactin* producing strains, with a critical value for the onset of surfing (triangles) at $\mathrm{Bo}_c^{\mathrm{bact.}} \approx 0.03 - 0.05$. The supernatant solution (SN) from an OD ≈ 0.27 suspension, and the commercial surfactin droplets ($0.1\,\mathrm{g\,l^{-1}}$) do not reach this value and no surfing is observed.

humidity in the climate chamber commonly used in swarming experiments, the gel slowly evaporates at a rate of about $\epsilon_{evap} \simeq 0.3\,\mu\mathrm{l\,h^{-1}\,cm^{-2}}$, as measured by weighing over a duration of 72 h. As time goes on, concentration gradients decrease as the surfactin molecules diffuse in the gel so that the inward osmotic flow decreases. Evaporation will eventually dominate, so that a drop only reaches a high enough Bond number and slides if its volume increase occurs within the first few hours of the experiment. Similarly, letting the gel dry in open air before the experiment makes it more difficult for bacteria to extract water out of the gel, hence limiting the overall volume increase of deposited drops (Fig. SF4). This probably explains why the active unpinning of bacterial droplets has never been reported before. On the contrary, no time limit should apply to colony surfing in saturated atmosphere, e.g. in the presence of a nearby water reservoir or in partially soaked porous media.

The volume increase of the droplet generates a proportional increase of gravitational pull, while capillary pinning forces increase only with the contact line length, which scales as $V^{1/3}$. The overall effect of the volume increase is thus to facilitate colony surfing by increasing the Bond number.

Lowering of the surface tension. The second mechanism that *B. subtilis* is able to harness directly impacts the capillary forces through a surfactant-induced reduction of surface tension. Thanks to the precision of our profilometric data, we can extract the curvature of the drops at different heights and infer the drop's surface tension *in situ* during the experiment. This shows that the constantly produced *surfactin* molecules lower the drop's surface tension by almost a factor 2 (Fig. 6). This decrease of surface tension generates a further increase of the Bond number (Eq. 1) by a similar factor.

We show in Fig. 7 the overall variation of the Bond number of 2 µl drops with different initial concentrations of bacteria. The Bond number increases significantly over time for high initial optical densities, OD ≈ 0.2 or higher, reaching about ten times its initial value. Colony surfing (onset marked by triangle symbols) is observed for a threshold value of $\mathrm{Bo}_c^{\mathrm{bact.}} \approx 0.03$ to 0.05, a value that is never reached by the supernatant solution or drops showing even less volume increase. This establishes a relation between the *surfactin* production, volume increase and the possibility of gravitationally driven onset of motion. Note, however, that the Bond number at which colony surfing is seen remains one order of magnitude below the critical Bond number of water which shows that the volume increase and the reduction of surface tension are only part of the toolkit available to *B. subtilis* for depinning its containing drop.

Enhancing the substrate wettability. Indeed, the production of surfactin also strongly enhances the wettability of the agar gel. The surfactant ring (SR) extending around drops containing surfactants marks the outer limit of the region of enhanced wettability (Figs. 1 and 3). Within the SR, contact angles of deposited water drops are dramatically lowered (27). Indeed when we place a large drop of water (30 µl), whose Bond number is below $\mathrm{Bo}_c^{\mathrm{H_2O}}$, next to a colony of non-motile, *surfactin*-producing bacteria (strain OMG 954), the water drop first remains immobile. When reached by the SR, it however starts sliding in the region of larger wettability (Supplementary Fig. SF2 and movie SM4).

To quantify the capacity of the agar gel surface to *pin* drops, we extracted the advancing and receding contact angles of sliding bacterial drops from our profilometric data. For a $V = 15\,\mu\mathrm{l}$ drop, of width $w = 12.5$ mm, we obtain $\theta_A \approx 6.5°$ and $\theta_R \approx 1.9°$, corresponding to a slope of 0.114 and 0.033, respectively (Supplementary Fig. SF3). The capillary pinning force which opposes the gravitational pull is directly proportional to $\Delta \cos\theta = \cos\theta_R - \cos\theta_A$. Drop sliding is thus only possible when the gravitational pull overcomes a critical value (28):

$$\rho V g \sin\alpha = w\gamma(\cos\theta_R - \cos\theta_A). \qquad [2]$$

This is equivalent to saying that the critical Bond number is $\mathrm{Bo}_c = \frac{w}{V^{1/3}}\Delta\cos\theta \simeq 0.03$ which is very close to the measured Bond number at which colony surfing is observed in our experiments (Fig. 7). This third mechanism thus concludes our discussion on the depinning of *B. subtilis* droplets seen in our experiments by providing a quantitative match with the corresponding critical Bond number.

Surfactin drops. To test more quantitatively the role of *surfactin*, we quantified its concentration in the supernatant of bacterial suspensions through High Performance Liquid Chromatography (HPLC, see *Materials and Methods* and suppl. Fig. SF9 and Table ST1). For a liquid culture of the SSB 1071 strain at OD $= 0.27$, we measured a surfactin concentration of $106(32)\,\mathrm{mg\,l^{-1}}$. We then compared the behaviour of a droplet

of the supernatant of this bacterial suspensions with a drop of commercial *surfactin* in water at a concentration of 100 mg l^{-1}. We show in Fig 5, 6, and 7 that their evolutions are very similar. Together with the experiments on the surfactin deficient strain 168, this shows surfactin to be the main tool used by *B. subtilis* to depin the droplets. Note that even higher concentrations of *surfactin* can even induce a depinning of the contact line. This however does not lead to a sustained motion of the droplet due to the finite extent of the surfactin ring in the absence of continuous production of surfactin by bacteria inside the droplet (Suppl. movie SM5).

Discussion

In this article, we have shown how *B. subtilis* colonies can modify their environment, creating a mobile drop which propels them across solid substrates at high velocities (3.1 cm h^{-1} on a 1° slope in supplementary movie SM3, potentially much more on steeper slopes), faster than any other surface-bound translocation mechanism described so far. Our measurements reveal that the bacteria have at least three distinct physico-chemical mechanisms they can use to this end: Liquid is extracted from the environment, inflating the drop and increasing the gravitational pull, the surface tension is lowered, and the wettability of the environment is significantly increased. This leads to a situation where the bacterial drop starts to run downhill on very shallow slopes, as low as 0.1°, under a gravitational pull which is two orders of magnitude too weak to depin a similar drop of water. While the influence of surfactant production on bacterial translocation has been observed in the context of flagellated swarming (15, 27, 29–32), or on biofilm spreading in liquid culture (33), this is to our knowledge the first observation of a surfactant-induced translocation mode where individual motility is not required. Its efficiency, making *colony surfing* the fastest surface translocation mode, is therefore even more remarkable, and arguably relevant in nature. Indeed, colony surfing can also occur if only part of the various mechanisms we uncovered are at play: a small bacteria-laden drop suspended on the upper plate of a sealed plastic box containing a water reservoir can undergo sliding while water droplets of similar sizes would remain stuck by capillary forces (SF10). Osmotic-induced surfing should thus be a rather generic phenomenon in humid environment. Furthermore, the exploitation of the physico-chemistry of surfactants to facilitate wetting and translocation will also be relevant in habitats with strongly varying humidity, such as soils (34) where surfactant-producing bacteria are rather common (35). Capillary forces are indeed known to control the water flow in porous media (36) so that collective surfing could strongly enhance migration speeds and distances of bacterial colonies through the soil pore network.

Materials and Methods

Volume and surface tension measurement. *In situ* volume and surface tension measurements are performed via a Moiré grid method where we calculate the free surface deformation from the distortion of the image of a grid modulating light intensity, as seen through the drop (18). In our set-up the grid translates uniformly, so that the intensity at every pixel varies periodically in time. A tilt in the air-drop or air-gel interface causes an apparent shift of the grid because of light refraction, producing a phase shift in the intensity signal. This shift can be precisely measured and related to the local interface slope through Snell's law. We use two perpendicular grids to measure two orthogonal slopes $h_x(x,y)$ and $h_y(x,y)$ simultaneously. The full surface profile $h(x,y)$ is obtained by a Fourier-transform integration (Frankot-Chellappa), and further integration $V = \int_S h(x,y)\,\mathrm{d}x\,\mathrm{d}y$ gives the drop volume. Conversely the derivatives h_{xx}, $h_{xy} = h_{yx}$ and h_{yy} yield the mean interface curvature κ:

$$\kappa = \frac{h_{xx}(1+h_y^2) + h_{yy}(1+h_x^2) - 2h_{xy}h_xh_y}{(1+h_x^2+h_y^2)^{3/2}}.$$

This curvature gives rise to a pressure jump across the air-drop interface, which in our very slow drops (Ca $< 10^{-6}$) depends only on height because hydrostatic pressure gradients in- and outside the drop are different (37):

$$\gamma\kappa(x,y) = p_0 + \rho g h(x,y).$$

With p_0 a constant, ρ essentially the density of water and the gravitational acceleration g known, the surface tension γ is immediately obtained from the slope of a linear fit of our measured interface height vs. curvature data. Calibration of the setup and subsequent algorithms is achieved by comparing the determined values for volume V, apex height $h^{\max}$ and curvature κ of various spherical-cap lenses with the manufacturer's specifications. Deviations are found to be within a 1 % margin. Furthermore, surface tension measurements on water, glycerol and surfactin solution were found to agree with measurements through the pendent drop method (38) to within 2 %.

Contact-angle determination. The contact line position is determined by noting that the second derivatives h_{xx} and h_{yy} of the height profile $h(x,y)$ must have a local maximum there, corresponding to the discontinuity at the triple liquid-solid-air interface (Fig. SF3). This yields the closed contact line around the drop with a precision of a few pixels, or about 1 % of a drop diameter of 5 mm to 15 mm at an image scale of 41.1 px/mm. The determined contact-angle measurements are again calibrated by comparison with the known border-gradients $h^{\max}_{x,y}$ of spherical cap lenses and show good agreement within a 5 % range.

Agar gel preparation. A 1.4 % (mass) stock solution is prepared from granular Agar (Difco). Just before an experiment, this solution is heated by microwave radiation until reaching the boiling point of water. The molten gel is weighted and solvent-loss due to evaporation is compensated for. We mix it with a liquid synthetic nutrient B-medium (39) (prepared at twice the final concentration) at a 1:1 ratio to obtain a 0.7 % gel solution with nutrients, from which 25 ml are poured in a Petri dish whose lid is closed immediately afterwards. Subsequent gelling takes place at constant temperature (30 °C) and on a flat surface for 20 min. The lid is then removed for a duration t_d (1 min unless specified otherwise) to dry the solidified gel surface in ambient air (RH=35 %). The process of drop deposition and transfer may add up to one minute to this open-lid drying time.

Bacterial strains and preparation. The *B. subtilis* strains (Laboratory strain 168, genotype *trpC2 swrA sfp*$^-$; SSB 1071, which is strain 168 restored to *sfp*$^+$ on the *thrC* locus, also known as OMG 930 (40); OMG 954, non-flagellated by deletion of the *hag* gene from SSB 1071 (40)) are taken from a −80 °C storage, spread out on a solid 0.7 % Agar medium with LB broth and antibiotics (SSB 1071: erythromycine 0.5 µg ml^{-1}, lincomycin 12.5 µg ml^{-1}; in the case of OMG 954 additionally chloramphenicol 5 µg ml^{-1}), and incubated at 30 °C and 70 %RH for 24 h. Microcolonies are taken from this gel and grown overnight in liquid B-antibiotics culture at 37 °C. The suspension is then diluted to an optical density (OD at 600 nm) of 0.1, and after 1 h a second time to OD = 0.1. It is left in the shaker until bacterial growth saturates. The doubling time in B medium at 30 °C resp. 37 °C is around 100 min resp. 85 min for strain 168, and 110 min resp. 90 min for SSB 1071 (Fig. SF6). 2 h to 4 h after departing from exponential growth, 2 µl drops of suspension (diluted to the desired OD) are deposited on the previously prepared agar gel and transfered into a constant climate chamber (Memmert HPP 110) at controlled humidity and at a temperature of 30 °C.

An optical density of OD = 0.27 corresponds to 10^8 cell/ml, i.e. a volume fraction $\Phi \simeq 0.05\,\%$.

Determination of surfactin concentration by HPLC. Concentrations of surfactin in surfactin-producing bacteria suspensions sampled from bulk and droplets deposited on gel were determined by reverse-phase C_{18} HPLC on a Varian Prostar equiped with a UV 320 detector by reference to a commercial surfactin standard (Surfactin from *B. subtilis*, 98 % pure, Sigma-Aldrich, batch n° 086K4109). The culture medium, as well as supernatant from a liquid culture of strain 168 which does not produce surfactin were also analysed as controls.

Acquisition of calibration data. A $1.3\,\mathrm{g\,l^{-1}}$ mother solution of commercial surfactin was prepared by dissolving 1.3 mg surfactin in 1 ml Ethanol (95 %). The mother solution was then diluted in MilliQ water to prepare calibration standards with 10, 100, 200, $300\,\mathrm{mg\,l^{-1}}$ concentrations. 100 µl samples were injected and eluted during 30 min using a mobile phase made of ACN/H_2O 80:20 (v/v) supplemented with 0.1 %(v) of trifluoroacetic acid, at a flow rate of $1\,\mathrm{ml\,min^{-1}}$. Detection was performed by measuring the absorbance at 205 nm.

Acquisition of sample data. Samples were filtrated on 0.2 µm cellulose acetate syringe filters, injected as 20 µl aliquots and eluted using the settings described for calibration standards.

Building of the calibration model and estimation of concentration in samples. Surfactin exists in several isomeric forms that usually coexist in the same extract. The proportions of the various isomers vary from one bacterial species to the other (Fig. SF8). Hence, for calibration, a global surfactin-correlated signal was built by summing the contributions of several isomers to the chromatogram. The peaks at 14, 18, 19 and 23.5 min were fitted to Gaussian curves, integrated and summed to give rise to a total surfactin signal that was plotted against the concentrations of the surfactin standards (Fig. SF9). A linear calibration model was built using the standards up to $300\,\mathrm{mg\,l^{-1}}$. It had a multiple R-squared correlation coefficient of 0.985 with a residual standard error of 0.0026 on 5 degrees of freedom. The limit of detection (LOD) was calculated with the usual definition of the concentration corresponding to the signal of the blank sample plus three standard deviation of the blank. The LOD was $44\,\mathrm{mg\,l^{-1}}$. Next, the equivalent concentrations of surfactin in the samples and controls were determined from the total surfactin-correlated peak areas of the corresponding chromatograms.

ACKNOWLEDGMENTS. We thank J.-F. Berret, M. Costalonga, C. Cottin-Bizonne, B. Desmazières, L. Hamouche, K. Hamze, I. B. Holland, S. Séror and M. Zhao for fruitful discussions. We thank David Clainquart and Marie-Evelyne Pinart from the Chemistry department of the University Paris Diderot for their assistance on the HPLC platform. This research was funded through the ANR grant *Bactterns*, CNRS grant PEPS "Micromanipulation de particules actives" and CNRS grant PIR "Mécanismes physiques et biologiques de la migration en masse de B. subtilis".

1. Wensink HH, et al. (2012) Meso-scale turbulence in living fluids. *Proceedings of the National Academy of Sciences* 109(36):14308–14313.
2. López D, Vlamakis H, Kolter R (2010) Biofilms. *Cold Spring Harbor Perspectives in Biology* 2(7).
3. Bridier A, Briandet R, Thomas V, Dubois-Brissonnet F (2011) Resistance of bacterial biofilms to disinfectants: a review. *Biofouling* 27(9):1017–1032. PMID: 22011093.
4. Budrene E, Berg H (1991) Complex patterns formed by motile cells of escherichia coli. *Nature* 349(6310):630–633.
5. Brenner MP, Levitov LS, Budrene EO (1998) Physical mechanisms for chemotactic pattern formation by bacteria. *Biophysical Journal* 74(4):1677–1693.
6. Cates M, Marenduzzo D, Pagonabarraga I, Tailleur J (2010) Arrested phase separation in reproducing bacteria creates a generic route to pattern formation. *Proceedings of the National Academy of Sciences* 107(26):11715–11720.
7. Liu C, et al. (2011) Sequential establishment of stripe patterns in an expanding cell population. *Science* 334(6053):238–241.
8. Hall-Stoodley L, Costerton JW, Stoodley P (2004) Bacterial biofilms: from the natural environment to infectious diseases. *Nature Reviews Microbiology* 2(2):95–108.
9. Berg HC (2008) *E. coli in Motion.* (Springer Science & Business Media).
10. Drescher K, Dunkel J, Cisneros LH, Ganguly S, Goldstein RE (2011) Fluid dynamics and noise in bacterial cell–cell and cell–surface scattering. *Proceedings of the National Academy of Sciences* 108(27):10940–10945.
11. Tuval I, et al. (2005) Bacterial swimming and oxygen transport near contact lines. *Proceedings of the National Academy of Sciences of the United States of America* 102(7):2277–2282.
12. Zhang R, Turner L, Berg HC (2010) The upper surface of an escherichia coli swarm is stationary. *Proceedings of the National Academy of Sciences* 107(1):288–290.
13. Fujikawa H, Matsushita M (1989) Fractal growth of bacillus subtilis on agar plates. *Journal of the physical society of japan* 58(11):3875–3878.
14. Ben-Jacob E, et al. (1994) Generic modelling of cooperative growth patterns in bacterial colonies. *Nature* 368(6466):46–49.
15. Harshey RM (2003) Bacterial motility on a surface: many ways to a common goal. *Annual Reviews in Microbiology* 57(1):249–273.
16. Julkowska D, Obuchowski M, Holland IB, Séror SJ (2004) Branched swarming patterns on a synthetic medium formed by wild-type bacillus subtilis strain 3610: detection of different cellular morphologies and constellations of cells as the complex architecture develops. *Microbiol.* 150(6):1839–1849.
17. Lee K, Ivanova N, Starov V, Hilal N, Dutschk V (2008) Kinetics of wetting and spreading by aqueous surfactant solutions. *Advances in colloid and interface science* 144(1):54–65.
18. Banaha M, Daerr A, Limat L (2009) Spreading of liquid drops on agar gels. *The European Physical Journal Special Topics* 166(1):185–188.
19. Arima K, Kakinuma A, Tamura G (1968) Surfactin, a crystalline peptidelipid surfactant produced by bacillussubtilis: Isolation, characterization and its inhibition of fibrin clot formation. *Biochemical and biophysical research communications* 31(3):488–494.
20. Peypoux F, Bonmatin J, Wallach J (1999) Recent trends in the biochemistry of surfactin. *Applied Microbiology and Biotechnology* 51(5):553–563.
21. Debois D, et al. (2008) In situ localisation and quantification of surfactins in a bacillus subtilis swarming community by imaging mass spectrometry. *Proteomics* 8(18):3682–3691.
22. Nikola N, et al. (2016) Active particles with soft and curved walls: Equation of state, ratchets, and instabilities. *Phys. Rev. Lett.* 117(9):098001.
23. Humphrey D, Duggan C, Saha D, Smith D, Käs J (2002) Active fluidization of polymer networks through molecular motors. *Nature* 416(6879):413–416.
24. Kajiya T, et al. (2013) Advancing liquid contact line on visco-elastic gel substrates: Stick-slip vs continuous motions. *Soft Matter* 9:454–461.
25. Cohen Stuart MA, de Vos WM, Leermakers FAM (2006) Why surfaces modified by flexible polymers often have a finite contact angle for good solvents. *Langmuir* 22(4):1722–1728.
26. Sokolov A, Goldstein RE, Feldchtein FI, Aranson IS (2009) Enhanced mixing and spatial instability in concentrated bacterial suspensions. *Physical Review E* 80(3):031903.
27. Leclère V, Marti R, Béchet M, Fickers P, Jacques P (2006) The lipopeptides mycosubtilin and surfactin enhance spreading of bacillus subtilis strains by their surface-active properties. *Archives of microbiology* 186(6):475–483.
28. Dussan V. EB, Chow RTP (1983) On the ability of drops or bubbles to stick to non-horizontal surfaces of solids. *Journal of Fluid Mechanics* 137:1–29.
29. Julkowska D, Obuchowski M, Holland IB, Séror SJ (2005) Comparative analysis of the development of swarming communities of bacillus subtilis 168 and a natural wild type: critical effects of surfactin and the composition of the medium. *Journal of bacteriology* 187(1):65–76.
30. Partridge JD, Harshey RM (2013) Swarming: flexible roaming plans. *Journal of bacteriology* 195(5):909–918.
31. Be'er A, et al. (2009) Paenibacillus dendritiformis bacterial colony growth depends on surfactant but not on bacterial motion. *Journal of bacteriology* 191(18):5758–5764.
32. Henrichsen J (1972) Bacterial surface translocation: a survey and a classification. *Bacteriological reviews* 36(4):478.
33. Angelini TE, Roper M, Kolter R, Weitz DA, Brenner MP (2009) Bacillus subtilis spreads by surfing on waves of surfactant. *Proceedings of the National Academy of Sciences* 106(43):18109–18113.
34. Or D, Smets B, Wraith J, Dechesne A, Friedman S (2007) Physical constraints affecting bacterial habitats and activity in unsaturated porous media – a review. *Advances in Water Resources* 30(6-7):1505–1527.
35. Bodour AA, Drees KP, Maier RM (2003) Distribution of biosurfactant-producing bacteria in undisturbed and contaminated arid southwestern soils. *Applied and Environmental Microbiology* 69(6):3280–3287.
36. Sadjadi Z, Rieger H (2013) Scaling theory for spontaneous imbibition in random networks of elongated pores. *Phys. Rev. Lett.* 110(14):144502.
37. De Gennes PG, Brochard-Wyart F, Quéré D (2013) *Capillarity and wetting phenomena: drops, bubbles, pearls, waves.* (Springer Science & Business Media).
38. Daerr A, Mogne A (2016) Pendent drop: An imagej plugin to measure the surface tension from an image of a pendent drop. *J. Open Res. Software* 4(1).
39. Antelmann H, et al. (1997) Expression of a stress-and starvation-induced dps/pexb-homologous gene is controlled by the alternative sigma factor sigmab in bacillus subtilis. *J. Bact.* 179(23):7251–7256.
40. Hamze K, et al. (2009) Identification of genes required for different stages of dendritic swarming in bacillus subtilis, with a novel role for phrc. *Microbiology* 155(2):398–412.

Supplementary information

Movies can be viewed online at http://www.msc.univ-paris-diderot.fr/~daerr/research/colonysurfingmovies.html or at http://www.pnas.org/content/suppl/2017/05/23/1703997114.DCSupplemental; click on the still pictures to open movie.

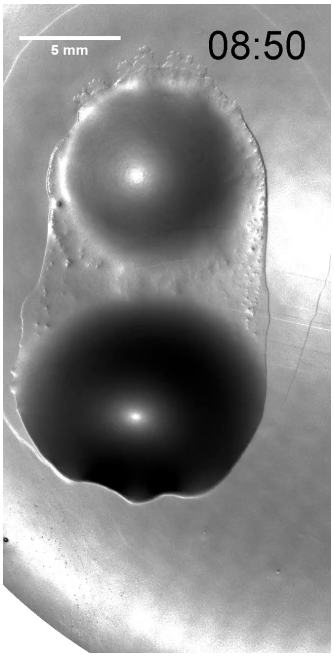

Movie SM1: Movie of a colony surfing event of a 2 µl drop (OD = 0.27) on a 1° slope (corresponding to main article figure 1). Time is indicated in hours:minutes, the time interval between two frames is 5 min.

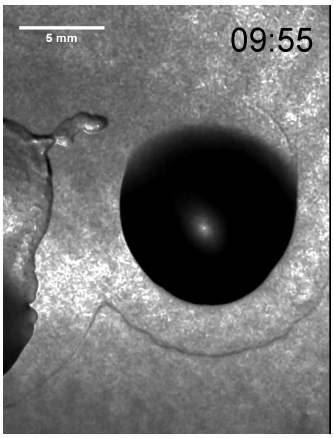

Movie SM2: Movie showing induced drop sliding of a 10 µl *supernatant* drop (right) contaminated by a dendrite of swarming bacteria from a 1 µl drop of bacteria (OD = 1.5, left) at $t \simeq 10$ h. The inclination angle is 1°. See main article figure 3 for details. Time is indicated in hours:minutes, the time interval between two frames is 5 min.

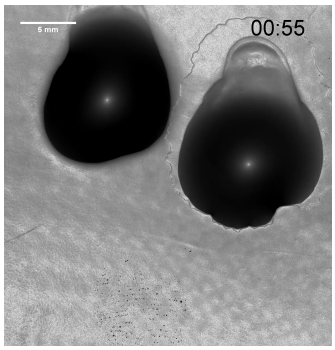

Movie SM3: Movie showing induced drop sliding of a 50 µl *water* drop (left) contaminated by a dendrite of swarming bacteria from a 30 µl drop of bacteria (right) at $t \simeq 110$ min. Here, to reduce initial drop spreading, the initial amount of *surfactin* present in the drop was minimised through the following procedure: the bacterial suspension was grown to OD = 1.5 and centrifuged; the supernatant was removed and the bacteria resuspended in fresh nutrients (final OD = 1.5) before deposition. The inclination angle is 1°. See supplementary figure SF1 for details. Time is indicated in hours:minutes, the time interval between two frames is 2.5 min.

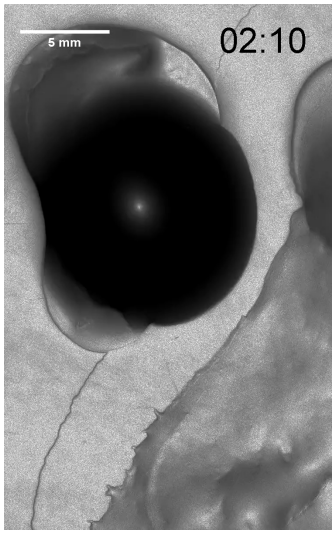

Movie SM4: Movie showing how a 30 µl water drop (left) starts to slide after being reached by the *surfactin* ring emitted by a 30 µl drop of non-motile bacteria (right). As for movie SM3, to reduce initial drop spreading, the initial amount of *surfactin* present in the drop was minimised through the following procedure: the bacterial suspension was grown to OD = 1.5 and centrifuged; the supernatant was removed and the bacteria resuspended in fresh nutrients (final OD = 1.5) before deposition. See supplementary figure SF2 for details. Time is indicated in hours:minutes, the time interval between two frames is 2.5 min.

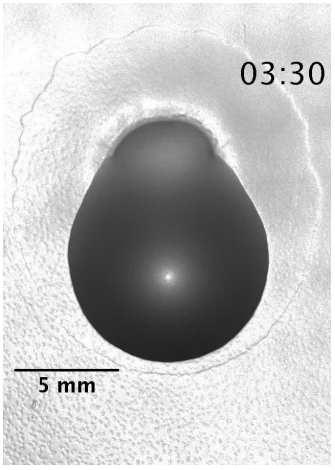

Movie SM5: Movie showing the evolution of a 2 µl drop of commercial *surfactin* solution ($0.5\,\mathrm{g\,l^{-1}}$) on the gel surface. As for bacterial suspensions, we observe a volume increase, and the outward propagation of a *surfactin* ring. The wetting hysteresis is reduced to $\Delta\cos\theta = \cos\theta_R - \cos\theta_A = 0.003$ at the onset of motion. As opposed to the drops of bacterial suspension the drop moves only through a finite distance, probably because sustained *surfactin* production is required to continuously modify the wetting properties of the gel ahead of the sliding drop. Time is indicated in hours:minutes, the time interval between two frames is 5 min.

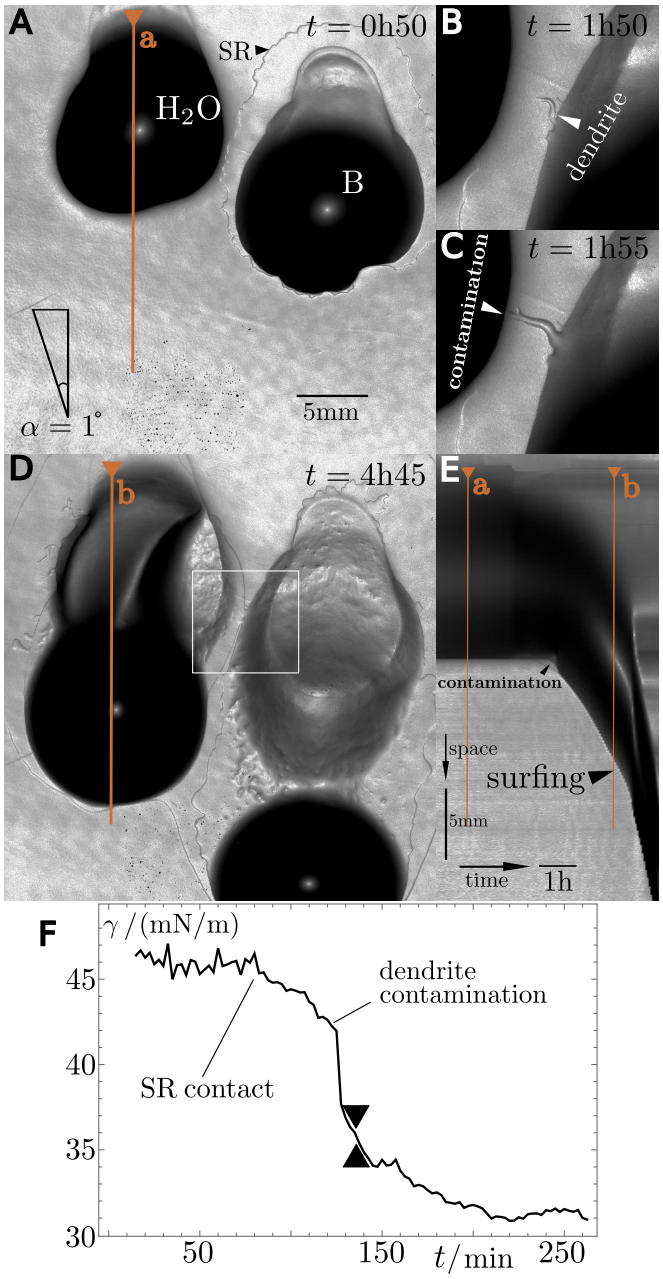

Figure SF1: **(A-D)** Snapshots of induced colony surfing, where the grey-level indicates the local slope. The right drop is a 30 µl drop of bacterial suspension (OD = 1.5), while the left drop is 50 µl of distilled water. The water drop starts to slide upon being contaminated by a dendrite of swarming bacteria (detail at 1 h 50, white rectangle region). **(E)** Kymograph of a cut through the water drop along the direction of motion showing the onset of sliding immediately after the contamination (black triangle). **(F)** Surface tension of the water drop. The surface tension starts decreasing from the moment the drop is reached by the *surfactin*-ring, indicative of surfactant molecules populating the interface. A much sharper decrease is associated with the contamination of the drop by a dendrite of migrating bacteria.

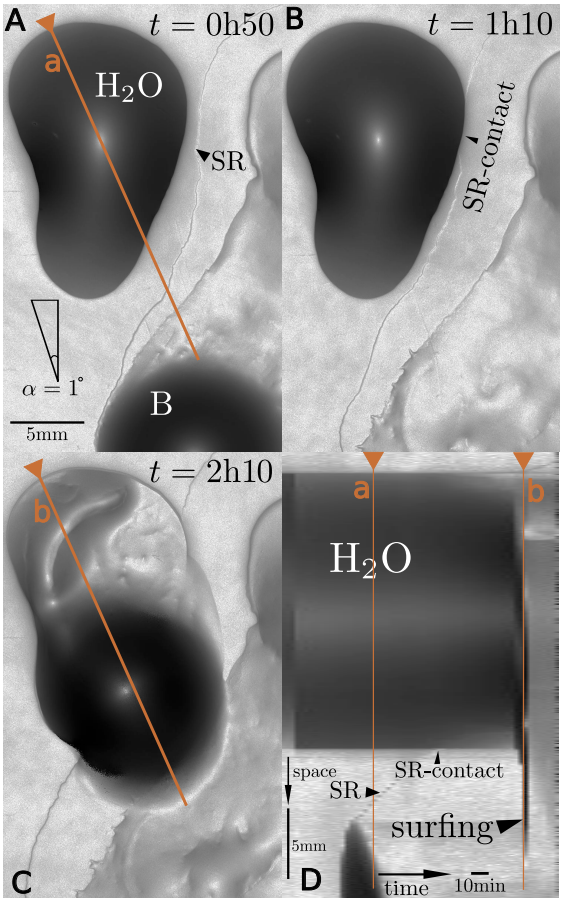

Figure SF2: **(A-C)** Snapshots of induced colony surfing, where the grey-level indicates the local slope. The right drop is a 30 µl drop of bacterial suspension (OD = 1.5), while the left drop is 30 µl of distilled water. The water drops starts to slide some time after the surfactant ring SR issued by the bacteria-laden drop reaches it, $t = 1\text{h}50$. **(D)** Kymograph of a cut through the water drop along the direction of motion showing the sudden onset of sliding around 40 min after contact with the SR.

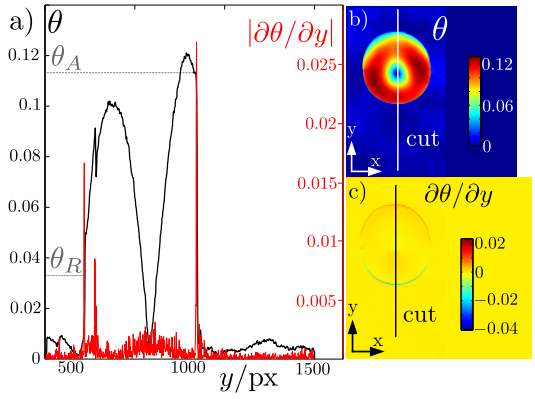

Figure SF3: Local contact line position and angles for a drop at the onset of colony surfing (corresponding to main article fig. 1). **(a)**: The advancing and receeding contact angles are determined as the intersection of the linear extrapolation of the free surface slope $\theta(y)$ to the position of the contact line given by the local maxima of the red curve. Here $\Delta \cos\theta = \cos\theta_R - \cos\theta_A \simeq 0.006$. **(b)** and **(c)**: Snapshot of the local angle of the free drop surface and of its derivative $\partial\theta/\partial y$ (top view).

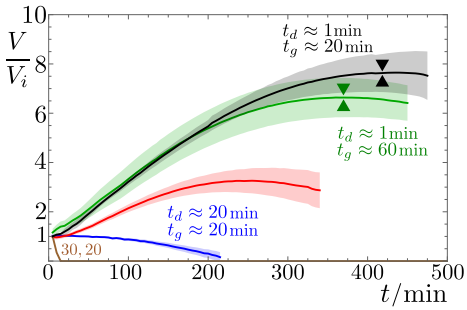

Figure SF4: Impact of gelling and drying time t_g, t_d on the inflation of deposited drops (OD = 0.27, $V_i = 2$ µl) measured by the relative volume increase V/V_i. On gels dried for 10 min, the volume gain V/V_i remains well below 4, half of the maximum volume gain for the shortest drying times. For drying times larger than about 20 min, the volume of deposited drops monotonically decreases. A longer *gelling* time (tripled from 20 min to 60 min) in turn has no significant effect on the evolution of deposited drops. Centerlines in saturated colors represent the mean value of a series of measurements, with the shaded regions around the curves indicating the standard deviation. Triangles mark the onset of colony surfing.

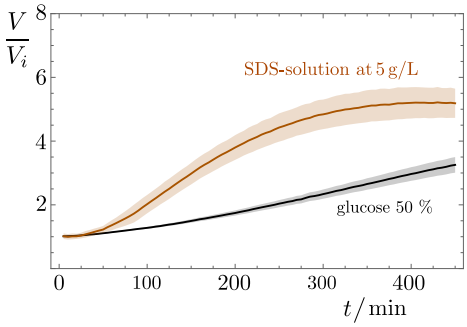

Figure SF5: Evolution of the volume of a glucose (50 % v/v) resp. a sodium dodecyl sulphate (SDS 5 g/l) drop at the gel surface after deposition at $t = 0$. The middle line in saturated color is the mean over several runs, the standard deviation being shown as shaded bands around the mean.

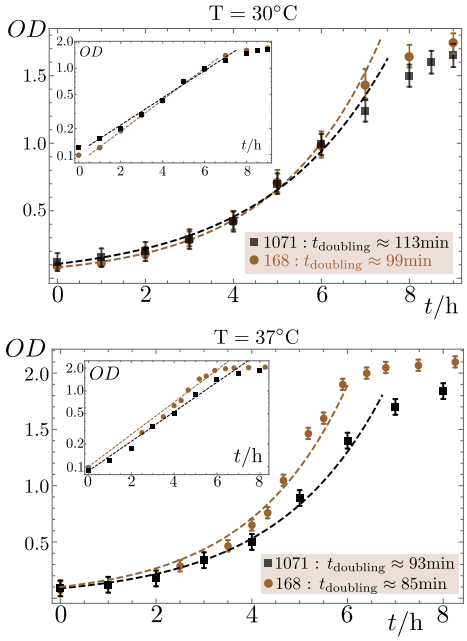

Figure SF6: The doubling time for bacteria grown with aeration in an agitated liquid B medium is estimated from optical density (OD) measurements at a wavelength of 600 nm. At a temperature

of 30 °C resp. 37 °C, we find around 100 min resp. 85 min for strain 168, and 110 min resp. 90 min for SSB 1071.

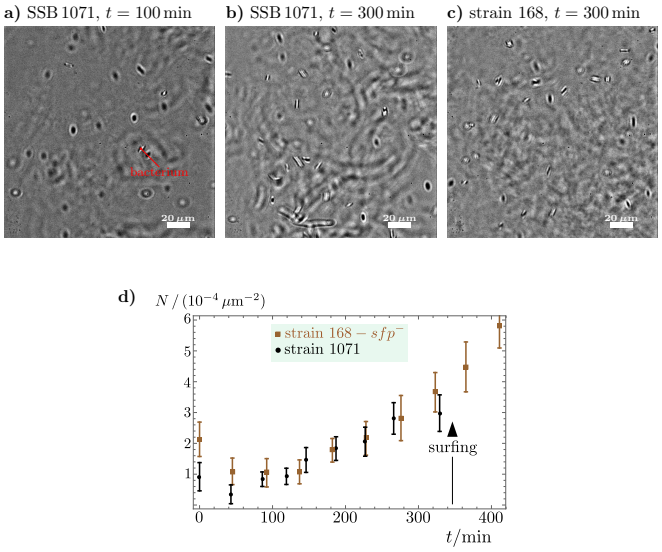

Figure SF7: Monitoring the bacterial concentration in sessile droplets (initially: $V = 5\,\mu$l, OD = 0.27) on agar (0.7 %, B medium, $T = 303\,$K, RH = 90 %) prior to colony surfing shows that the suspension remains dilute over the course of the experiment. **(a-c)** Microscope images at 40x magnification, focussed at mid-height in the drop ($z = 0.5h_{\max}, h_{\max} \simeq 0.3\,$mm). The depth of field is of the order of 1 µm. The bacterial concentration within the droplet remains very dilute even at $t = 300\,$min for both strains 168 and SSB 1071. **(d)** Mean density of bacteria in a slab such as shown in the top row of images (a-c), averaged across the droplet's height, i.e. over $\simeq 15$ to $\simeq 20$ slabs — depending on the droplet growth — recorded every 14 µm from top to bottom. The thickness of a slab is set by the depth of field, $\simeq 1\,\mu$m. No major increase in bacterial density is observed. Note that only strain SSB 1071 undergoes colony surfing (at $t \simeq 350\,$min).

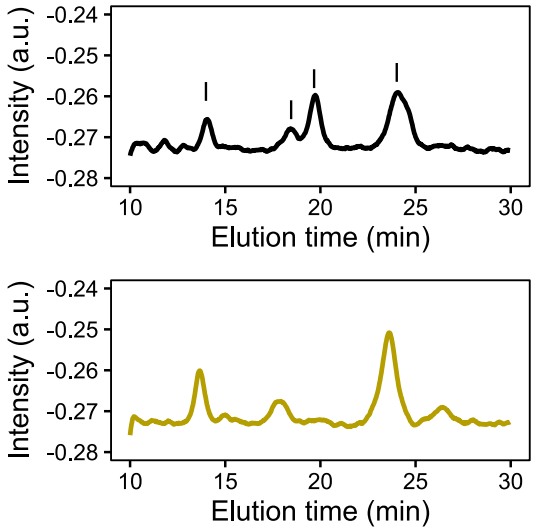

Figure SF8: Typical HPLC chromatograms of commercial *surfactin* (top) and *surfactin* produced by our *B. subtilis* strain SSB 1071 (bottom). The peaks highlighted in the commercial *surfactin* chromatogram were exploited for the construction of the calibration plot.

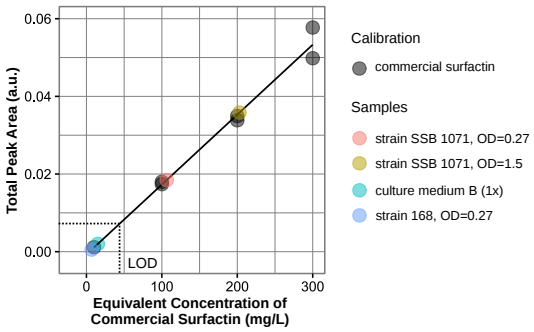

Figure SF9: Total *surfactin*-correlated peak intensity vs. commercial *surfactin* concentration calibration plot. LOD indicates the Limit Of Detection (see Materials and Methods).

Sample	Equivalent commercial concentration (90% confidence limits) (mg/L)
strain SSB 1071, OD=0.27	106(32)
strain SSB 1071, OD=1.5	202(32)
B(1x), culture medium	<44 ppm (below LOD)
strain 168, OD=0.27	<44 ppm (below LOD)

Table ST1: Surfactin concentration estimation from HPLC measurements. LOD indicates the Limit Of Detection (see Materials and Methods).

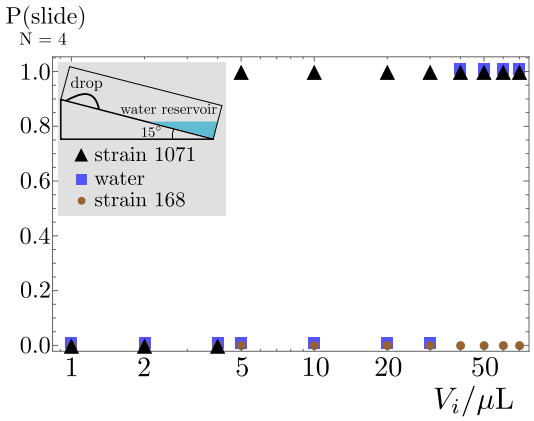

Figure SF10: Probability to observe colony surfing in a bare polystyrene Petri dish at 15° tilt, closed, and with a water reservoir at the bottom, as a function of the initial deposited volume. The surfactin producing strain SSB 1071 starts to slide at much smaller volumes ($V_i^{\mathrm{crit}} = 4\,\mu$l) when compared to water and the surfactin-deficient 168 strain. The experimental protocol closely follows that of the experiments on gel. The bacterial suspension is prepared using the same protocol (see Materials and Methods). Drops of different volume at an initial optical density of OD = 0.27 are deposited in an inclined clean polystyrene Petri dish placed inside a climate chamber (T=30 °C, RH=70 %). 10 ml of distilled water is added at the bottom of the dish as a source of humidity (see inset). Finally the Petri dish cover lid is put in place and the chamber is closed. Four drops were measured for each condition.